

---

NANOSCALE AND NANOSTRUCTURED  
MATERIALS AND COATINGS

---

## Electrocopolymerization, Characterization and Anticorrosive Properties of Nanostructure Poly (aniline-co-4-hydroxy phenyl acetic acid)

Hamid Zebhi<sup>a</sup>, Mohammad Hossein Heydari<sup>b,\*</sup>, Khalil Farhadi<sup>a</sup>, and Peyman Najafi Moghadam<sup>a</sup>

<sup>a</sup>Department of Chemistry, Faculty of Science, Urmia University, Urmia, Iran

<sup>b</sup>Department of Chemistry, Faculty of Science, University of Zanjan, Zanjan, Iran

\*e-mail: m.h.heydari.p@gmail.com

Received September 4, 2017; revised February 6, 2019; accepted March 9, 2019

**Abstract**—In this study electrochemical deposition of nanostructure poly (aniline-co-4-hydroxy phenyl acetic acid) (PAHPA), polyaniline (PANI) and poly (4-hydroxy phenyl acetic acid) (PHPA) were carried out using cyclic voltammetry (CV) in aqueous solution of oxalic acid 0.3 M as reaction medium to achieve a protective coating for ferritic and economic 430SS in high corrosive solutions as 3.5% NaCl. In the electropolymerization of PAHPA, the monomer ratio was 1 : 1 (mol/mol). FT-IR and CV techniques were applied to characterize electrodeposited coatings. The morphological and structure analyses of the deposited films were done using scanning electron microscopy (SEM). Anticorrosive behaviors of coated steels were investigated by two techniques, potentiodynamic polarization and EIS (Electrochemical Impedance Spectroscopy) and were compared with protection efficiencies of PANI and PHPA. Our results showed that PAHPA coatings provided a noticeable better corrosion protection than homopolymers. The protection efficiency value for the PAHPA coated 430SS electrode was 97%, that it was higher than protection efficiencies of the homopolymers. Also effect of long immersion times on the protective films and their corrosion behaviors was studied. The PAHPA protection efficiency decreased about %3 when immersion time increased to 10 days. These results demonstrated the copolymer film can be highly corrosion resistant coating for 430SS in corrosive solutions that have chloride ions.

**Keywords:** conducting polymers, poly(aniline-co-4-hydroxy phenyl acetic acid), polyaniline, poly(4-hydroxy phenyl acetic acid), electrochemical depositing

**DOI:** 10.1134/S2070205119050113

### INTRODUCTION

Conducting polymers (CPs) commonly are synthesized by two methods: electrochemical and chemical. First method is more advantageous than the second. The final products are clean and don't need for removing the reaction mixture. The CPs electro-deposition on the surface of metal electrodes is an interesting field for researchers due to the fact that they have excellent electrochemical characteristics, like sufficient electrochemical stability [1, 2], simple synthesis [3, 4], easy doping [5] and high electrical conductivity [6]. The mentioned characteristics lead CPs have been vigorously investigated due to their numerous potential applications in electro-chromic [7], microelectronic, photo-electronic and display devices [8, 9], sensors [10–12], biological applications [13], batteries [14, 15], chemically modified electrodes [16], fuel cells [17] anticorrosive film on metals [2, 3] etc.

Using these polymers for controlling corrosion progression in metals is a well-known and consequential potential application. Among CPs, polyaniline

(PANI) is one of the most studied polymers that applied as coating to corrosion inhibition [18, 19]. Also, its derivatives [20, 21], copolymers [22, 23] and “PANI/other CPs” multilayer systems [24, 25] have been investigated as protective coatings. Since the advent of the nanotechnology era, nanostructure CPs has been synthesized by various groups of researchers [25–27].

Stainless steels (SS) is an alloy that protect itself by creating a passive layer. It is believed that this layer is Cr<sub>2</sub>O<sub>3</sub> [28]. Therefore, SS has a notable corrosion resistance and is used in many industrial applications. In sailor environment, steel and steel alloys are mostly used as building materials due to their profits such as good mechanical properties, availability and low cost. Unhappily, in spite of these mentioned profits, these alloys are corroded in solutions that have chlorides like sea water [29]. Therefore, coating the SS substrates with a sufficient passive film is necessary before applying in the industry. Coating with electrodeposited CPs is a best known method for this purpose. Various SS

types, like 304 [30, 31], 304L [29], 316 [32], 316L [33], 410 [34], and 430 [35], have been used as substrates for CPs electropolymerization.

In the following of our works on electrodeposited anti-corrosive polyaniline and its derivations on the Ferritic 430 stainless steel (430SS) electrodes [19, 25], we carried out present investigation. This work had three aim. First, to achieve an adhering coating of the PAHPA using CV on the 430SS electrode. Second, polymer structure characterizing by electrochemical methods, SEM and FTIR techniques. Third, to investigate PAHPA coated steel electrode corrosion protection performance utilizing two techniques: potentiodynamic polarization and EIS (Electrochemical Impedance Spectroscopy) in 3.5% NaCl solutions and finally comparing protection efficiency of PAHPA, PANI and PHPA.

## EXPERIMENTAL

### Chemicals

Monomers (aniline and 4-hydroxy phenyl acetic acid) and oxalic acid were purchased from Merck (Germany). Before experiments, aniline was distilled two times and acquired colorless liquid was stocked in completely dark place at 5°C. 4-hydroxy phenyl acetic acid and oxalic acid were consumed without purification and doubly distilled water was used for aqueous solutions. The working electrode was 1 cm<sup>2</sup> 430SS that embedded in Teflon holder and pretreatment of its surface before each experiment was carried out according to our previous work [25].

### *Synthesis of poly (aniline-co-4-hydroxy phenyl acetic acid) (PAHPA), polyaniline (PANI) and poly (4-hydroxy phenyl acetic acid) (PHPA)*

The PAHPA copolymer coating was synthesized on 430SS substrate by applying CV. For the electrochemical copolymerization, a mixture of aniline and 4-hydroxy phenyl acetic acid with concentration of 0.1 M from each monomer was used in 0.3 M aqueous solution of oxalic acid. To obtain different thickness of coatings and investigation of its effect, the copolymer synthesis experiments were carried out by using different scan numbers as 5, 10 and 20. The synthesized copolymer coatings were abbreviated by taking into consideration the scan numbers used for the synthesis. For example, the copolymer coating synthesized with 5 scan was abbreviated as PAHPA5.

A simple three electrode cell was utilized with Ag/AgCl electrode as reference and counter electrode was 430SS plate. The working electrode was pretreated 430SS of area 1 cm<sup>2</sup>. An Autolab (USA) Potentiostat-Galvanostat (model: PGSTAT30) was used for maintaining conditions of cyclic voltammetry. The PAHPA was synthesized by continuously cycling of working electrode potential between -0.5–1.6 V for

first scan and from -0.5 to 1.2 for next scans (scan rate was 0.01 V/s). After CV cycles, the coated electrodes were removed from electrolyte and rinsed with bi-distilled water afterwards dried at 40°C.

PANI and PHPA were synthesized on 430SS electrodes similar to PAHPA. For PANI, solution contains 0.1 M aniline and 0.3 M aqueous oxalic acid. More explained details of PANI electropolymerization was reported in our previous study [25]. For PHPA, solution contains 0.1 M 4-hydroxy phenyl acetic acid monomer and 0.3 M aqueous oxalic acid. Electrochemical conditions were same for homopolymers and copolymer.

### Characterization

Characterization of electrochemically synthesized films was done by FTIR. These films were powdered first and then were compressed in KBr and spectra were recorded by a Thermo Nicolet spectrometer (USA), spectra were scanned from 4000 to 400 cm<sup>-1</sup>. Investigation of coatings surface morphologies was performed by scanning electron microscopy (SEM) XL-30, Philips (USA). Calculation of coating thickness is one of the important parameters for synthesis of the polymer coatings on the metal surface, which is an important feature for industrial applications. EIS data can be used for measurement of the thickness of conducting polymeric coatings. Coating thicknesses was achieved to the following equation by using CPE<sub>dl</sub> [36]:

$$CPE_{dl} = \epsilon_0 \epsilon A / d,$$

where  $\epsilon$  is the dielectric constant of the environment,  $\epsilon_0$  is the vacuum permittivity, A is the electrode area and d is the thickness of the protective coating layer.

### Corrosion Resistance Tests

Corrosion resistances of 430SS electrodes before and after films deposition were evaluated in 3.5% NaCl solution by two valid methods: electrochemical impedance spectroscopy (EIS) and potentiodynamic polarization (Tafel polarization). These experiments were done at room temperature. For obtaining constant value of open circuit potential (OCP), the electrodes were submerged in NaCl solution for 120 h prior to the potentiodynamic polarization and OCP values were monitored in this period. The potentials were swept with 1 mVs<sup>-1</sup> scan rate for Tafel polarization tests and potential range was  $\pm 250$  mV vs. OCP. All tests were repeated three times or more to achieve a repeatable result.

Various frequencies (10000–0.1 Hz) were impressed in the EIS measurements at OCP with 5 mV a.c signals. Zview software was used for fitting experimental data to equivalent circuits and impedance spectra analyzing.

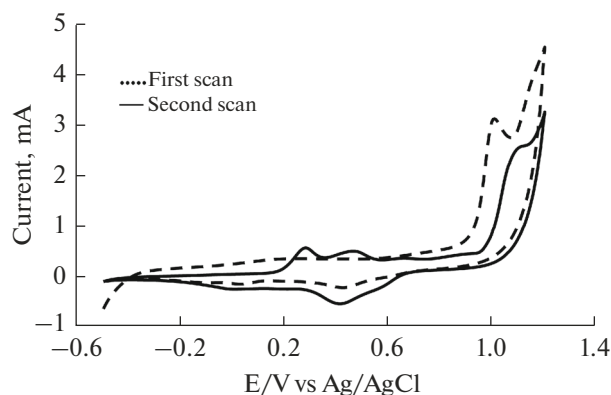


**Fig. 1.** Recorded cyclic voltammograms for 430SS electrode in the 0.3 M oxalic acid solution containing 0.1 M aniline and 0.1 M 4-hydroxy phenyl acetic acid (....) first scan; (—) second scan.

## RESULT AND DISCUSSION

### *Electrochemistry of Synthesis*

The PAHPA was deposited electrochemically on 430SS electrodes. The range of potential in the CV was  $-0.5$ – $1.2$  V. First and second of CVs are showed in Fig. 1. In the case of first scan curve, a current appears at  $-0.5$  and increases with sweeping to anodic potentials up to  $0.2$  V is belong to 430SS dissolution. This current becomes nearly constant from  $0.2$  to  $0.6$  V because of the formation of  $\text{Cr}_2\text{O}_3$  layer on the substrate surface. This protective prevents further substrate dissolution [37]. Increasing of current after  $0.6$  V suggests that  $\text{Cr}_2\text{O}_3$  film breaks down at this potential reign. A relatively sharp peak seems in  $1.0$  V which it's not exist in second scan. Disappearing of this peak confirms that it is attributed to the dissolution of 430SS substrate. Deposited copolymer film in first scan inhibits the further dissolution of 430SS surface during next scans. The peak that belongs to oxidation of aniline monomer appears in  $1.1$  V and approximately remains constant in the second and subsequent scans [38]. By the oxidation of aniline monomers, emeraldine (EM) and aniline/4-hydroxy phenyl acetic acid oligomers start to form and film nucleation initiates [39].

At the beginning of the second cycle anodic sweep, 430SS dissolution current is very slight ( $\sim 0.0$  V) till  $0.2$  V, because of the monomers adsorbing as corrosion inhibitors. Two peaks at about  $0.3$  and  $0.5$  V are due to the oxidations of leucoemeraldine (LE) into EM [31] and generated oligomers oxidation [20] respectively. A peak that occurs at  $0.98$  V and grows up in the subsequent scans, is as a result of EM oxidation to pernigraniline [40]. Further cycles of electropolymerization are represented in Fig. 2. As seen, by increasing the scans number, intensity of the LE and EM oxidation peaks are increasing that proves successive growth of the copolymer film on the 430SS substrate. Another

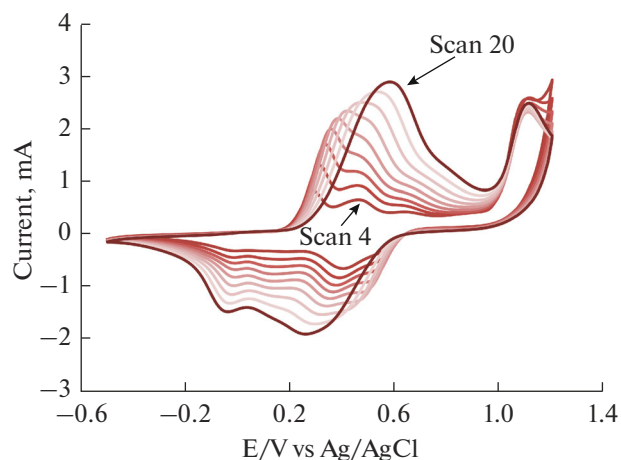


**Fig. 2.** Copolymerization cyclic voltammograms of aniline and 4-hydroxy phenyl acetic acid on 430SS electrode. (Scan rate  $10 \text{ mVs}^{-1}$ ).

evidence is the shifting of oxidation and reduction peaks to higher and lower potentials, respectively. Simultaneous increasing in the oxidation and related reduction peaks indicates the redox behavior of electrosynthesized copolymer.

### *FTIR studies of PAHPA*

The FTIR spectra of electropolymerized PAHPA20 film on 430SS electrode is presented in Fig. 3. The  $\text{C}=\text{C}$  and  $\text{C}=\text{N}$  stretching mode for the benzenoid and quinoid rings appear at  $1494$  and  $1577 \text{ cm}^{-1}$  [41]. 1,4-para substituted benzene ring's peak occurs at  $796 \text{ cm}^{-1}$  [42] that proves aniline monomer participated in the copolymer chain. The band at  $2925 \text{ cm}^{-1}$  is characteristic band for the stretching vibration of aromatic  $\text{C}-\text{H}$  [27]. The peak at  $1294 \text{ cm}^{-1}$  corresponds to  $\text{N}-\text{H}$  bending mode. The band that has medium intensity near  $1241 \text{ cm}^{-1}$  is assigned to  $\text{C}-\text{N}$  stretching mode for the benzenoid ring [42]. Functional groups of 4-hydroxy phenyl acetic acid monomer are  $\text{C}=\text{O}$  and  $\text{O}-\text{H}$ . If this monomer exists in the polymer backbone, the peaks of its functional groups must be in the spectra. The peaks at  $1690$  and  $3443 \text{ cm}^{-1}$  are related to presence of  $\text{C}=\text{O}$  and  $\text{O}-\text{H}$  groups, respectively [31]. Also, the peaks at  $702$  and  $1770$  are due to the ortho-substituted benzene ring which reveals 4-hydroxy phenyl acetic acid was copolymerized with aniline. Comparison of synthesized copolymer FTIR spectra with of the polyaniline [19] shows that these peaks are not observed in last one.

### *Surface Morphology Evaluations of Copolymer*

The template-free method, always called the soft template synthesis method or self-assembly method in the literatures [41], entails synthesizing the PANI in

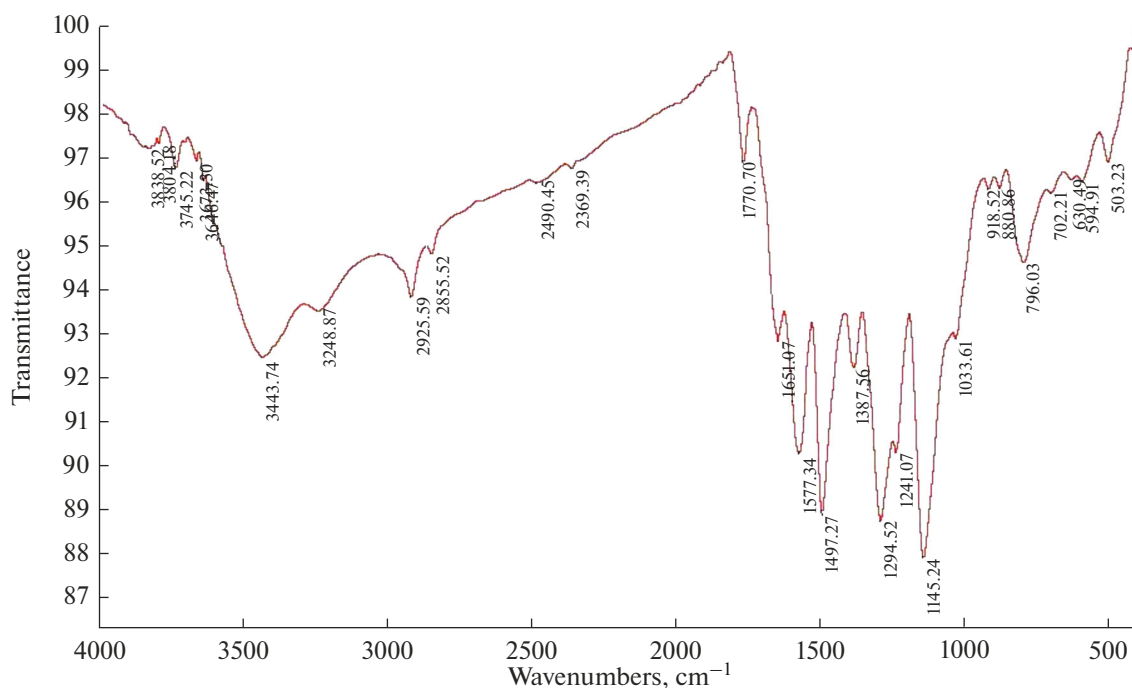


Fig. 3. FTIR spectrum for PAHPA20 coating deposited on 430SS.

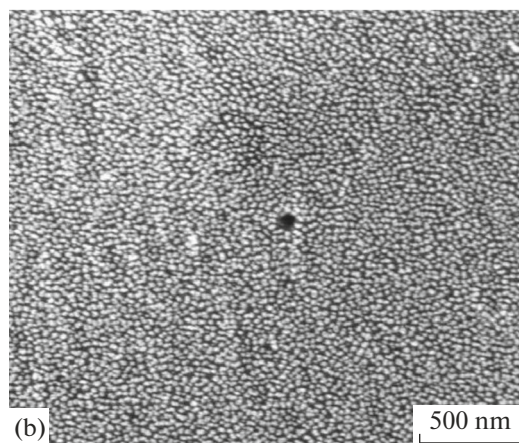
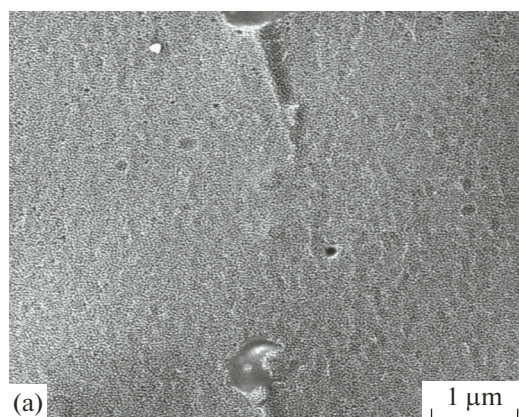


Fig. 4. SEM images of electrocopolymerized PAHPA on 430SS.

the presence of structure-guiding molecules such as polyelectrolytes [42] which act as surfactants and templates for production of the nanomaterial. The surfactants are often complex acids with bulky side groups, such as the naphthalene sulfonic acid [43], camphor-sulfonic acid [44], 5-aminonaphthalene-2-sulfonic acid [45], azobenzenesulfonic acid [46], etc.

In this study we were used from 4-hydroxy phenyl acetic acid for this mean and as comonomer for the synthesis of PANI copolymer. SEM images (Fig. 4) show that the prepared copolymer has nanostructure and extremely uniform morphology. Uniformity of morphology demonstrated that coating is copolymer not bilayer or other forms. One can compare these images with SEM images of bilayer system [44].

#### *Stability of PAHPA on 430SS*

It is confirmed that electrochemical degradation of conductive polymers occur when adequately high anodic potentials are applied. In order to investigate electrochemical stability and to obtain sufficient information about properties of the PAHPA20 coating, cyclic voltammetry was carried out in monomer free 1.0 M oxalic acid solution (Fig. 5). Resulted cyclic voltammograms show the redox property of PAHPA20 through its oxidation/reduction peaks and after 20 cycles, a trifling decrease in the peak intensities was observed. This result revealed that electrodeposited PAHPA film on the 430SS has sufficient adhesion to the surface of substrate and stable electroactivity after 20 cycles [38].

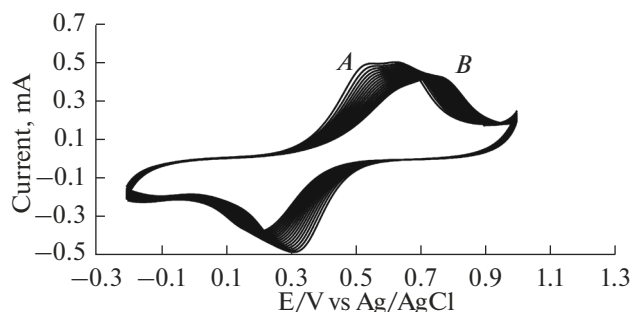


**Fig. 5.** Cyclic voltammograms of PAHPA coated 430SS in monomers free 1 M oxalic acid solution (scan rate  $10 \text{ mVs}^{-1}$ ) (A) first cycle and (B) 30th cycle.

These features are essential for an excellent corrosion protective coating.

#### Corrosion Protection Studies

All testing electrodes (uncoated and coated) were investigated to evaluate their ability to protect 430SS substrate against corrosion in 3.5% wt. NaCl solution using potentiodynamic polarization (Tafel) test and impedance spectroscopy technique.

#### Potentiodynamic Polarization Tests

Figure 6 shows the potentiodynamic polarization curves for bare, homopolymer and copolymer coated 430SS electrodes in 3.5% wt. NaCl solution. As seen in Fig. 6, a potential shift in corrosion potential ( $E_{\text{corr}}$ ) was obtained for all coated substrates with respect to that of the bare electrode. This confirms that all homopolymer and copolymer films are corrosion protective coatings (anodic protection) for 430SS surface. Another obvious feature is the decreasing in the corrosion current density ( $I_{\text{corr}}$ ) of the coated electrodes compared to that of the uncoated 430SS sample. Extracted parameters from Tafel curves are given in Table 1. The  $I_{\text{corr}}$  values decreased from  $6.665 \mu\text{A cm}^{-2}$  for bare 430SS to 0.187, 0.380 and  $0.926 \mu\text{A cm}^{-2}$  for PAHPA20, PANI20 and PHPA20 coated 430SS elec-

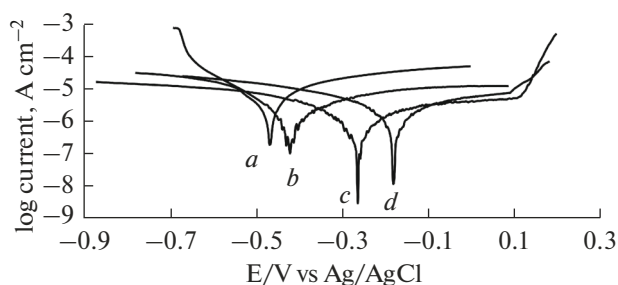


**Fig. 6.** Polarization behavior of uncoated and coated 430SS samples in 3.5% NaCl. (a) Bare steel, (b) PHPA20, (c) PAHPA20, and (d) PANI20.

trodes. The  $I_{\text{corr}}$  of the copolymer deposited sample is lower than those of the homopolymers. This interesting result shows that when a PAHPA20 coated 430SS substrate be immersed in to 3.5% wt. NaCl solution, it is very slowly corroded than bare and even PANI20 coated ones. Corrosion rates values (CR) in Table 1 confirm it. CRs were calculated by the relation [20]:

$$CR(\text{mm/y}) = 3.238 \times 1000 \frac{I'_{\text{corr}}}{\rho} E_w,$$

where  $I'_{\text{corr}}$ ,  $\rho$ ,  $E_w$  are corrosion current density for coated electrode ( $\text{A cm}^{-2}$ ), the 430SS density ( $\text{g cm}^{-3}$ ) and 430SS equivalent weight (g).

The CR of the copolymer coated 430SS substrate is the lowest among all and it is  $\sim 50$  times lower than obtained CR of the uncoated 430SS sample. This is an excellent result. The protection efficiency ( $\eta_p$ ) of the coatings has been calculated from the extrapolation of Tafel plots as [47]

$$\eta_p = \frac{I'_{\text{corr}} - I_{\text{corr}}}{I'_{\text{corr}}} \times 100,$$

where  $I'_{\text{corr}}$  and  $I_{\text{corr}}$  are the corrosion current densities of bare and coated 430SS electrodes, respectively.

The protection efficiency of PAHPA20 coating on the 430SS surface have been obtained about 97.2%

**Table 1.** Corrosion current ( $I_{\text{corr}}$ ), polarization resistance ( $R_p$ ), corrosion potential ( $E_{\text{corr}}$ ) and protection efficiency ( $\eta_p$ ) values calculated from Tafel plots for bare steel and electropolymerized PHPA20, PAHPA20 and PANI20 on 430SS samples in 3.5% NaCl solution

Sample	Film thickness, $\mu\text{m}$	$E_{\text{corr}}$ , V vs Ag/AgCl	$I_{\text{corr}}$ , $\mu\text{A cm}^{-2}$	$R_p$ , $\Omega\text{cm}^2$	$P$ , %*	CR, mm/y	$\eta_p$ , %
Bare steel	—	-0.47	6.655	$7.95 \times 10^3$	—	1.207	—
PANI20	0.76	-0.18	0.380	$2.63 \times 10^4$	2.84	0.063	94.3
PHPA20	1.29	-0.42	0.926	$2.43 \times 10^4$	3.01	0.162	86.0
PAHPA20	1.08	-0.27	0.187	$5.35 \times 10^4$	1.39	0.024	97.2

\*  $b_a = 0.322 \text{ V.dec}^{-1}$

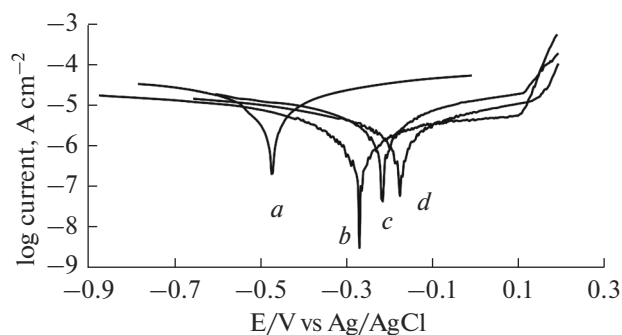


**Fig. 7.** Polarization behavior of electrocopolymerized PAHPA on 430SS in 3.5% NaCl. (a) Bare 430SS, (b) PAHPA20, (c) PAHPA10, and (d) PAHPA5.

that it is more than even PANI20 film. Porosity of coating is one of the most important factors that extremely influences on all anticorrosive properties of coatings. Potentiodynamic polarization results were used to determine the coatings porosity by the relation [30]

$$P = \frac{R_{p(unc)}}{R_{p(c)}} \times 10^{-(\Delta E/b_a)}$$

where  $P$  is the coating porosity,  $R_{p(c)}$  and  $R_{p(unc)}$  are the polarization resistance of the coated and uncoated substrate, respectively.  $\Delta E$  is the measured difference between the corrosion potentials and  $b_a$  is the anodic Tafel slope for the bare 430SS sample. Obtained value for Porosity of the copolymer was 1.39% and as expected it is lower than those of the both homopolymers. PANI has lower porosity than PHPA, because PHPA has large acetic acid side group. The low porosity of PAHPA20 is probably due to hydrogen bonds between H of the acetic acid group from one chain and N of the aniline group from other polymer chain. Consequently, the porosity effects on the corrosion protection, and PAHPA20 has best protection efficiency. On the other hand, porosity influences the adherence of coating on electrode. It was proved that PAHPA is more adherent than PANI and PHPA when removing coatings from electrodes surface by polishing coated samples with emery papers.

Further investigation was carried out to evaluate the dependence of anticorrosive behaviors to the protective film thickness. Different thicknesses of the copolymer were deposited on 430SS electrode and Tafel tests were done on them. Obtained results for this study are represented in Fig. 7 and Table 2. It was found that increment of electrodeposited film thickness effects on the  $I_{corr}$  and subsequently on the  $\eta_p$ . The  $I_{corr}$  and  $\eta_p$  values become lower and higher respectively, when the film becomes thicker.

#### Electrochemical Impedance Measurements

EIS measurements were carried out for evaluating the performance of coated and bare 430SS electrodes against corrosion. Figure 8 shows the Nyquist diagrams for the bare (Fig. 8a) and PHPA, PANI and PAHPA coated 430SS electrodes (Fig. 8b) in 3.5% wt. NaCl solution. Figure 9a represents equivalent circuit models for uncoated 430SS electrode that impedance data of bare electrode was fitted with it and includes the electrolyte resistance ( $R_s$ ), double layer capacitance ( $C_{dl}$ ) and charge transfer resistance ( $R_{ct}$ ). In fact,  $R_{ct}$  is the sum of these resistances: the charge transfer resistance at the metal/oxide film interface and oxide-film/solution interface [24, 38]. A constant phase element ( $CPE_{dl}$ ) was used instead of the  $C_{dl}$  to describe the deviation from the ideal behavior of capacitance.  $CPE_{dl}$  for bare 430SS depicts capacitance at the metal/solution interface. The constant phase element has been defined as [48]:

$$CPE = [Q(j\omega)^\alpha]^{-1},$$

where  $Q$ ,  $j$ ,  $\omega$  and  $\alpha$  are the frequency-independent constant, the imaginary unit (square =  $-1$ ), angular frequency and correlation coefficient of the CPE ( $0 < \alpha < 1$ , for an ideal capacitance:  $\alpha = 1$ ), respectively.

Also, the Nyquist plots of all coated samples were modeled using the equivalent circuit which is shown in Fig. 9b [49]. In this circuit,  $CPE_c$ ,  $CPE_{dl}$ ,  $R_s$ ,  $R_c$  and  $R_{ct}$  are the coating capacitance (capacitance at the metal/coating interface), double layer capacitance (capacitance at coating/solution interface), electrolyte

**Table 2.** Corrosion current ( $I_{corr}$ ), polarization resistance ( $R_p$ ), corrosion potential ( $E_{corr}$ ) and protection efficiency ( $\eta_p$ ) values calculated from Tafel plots for bare steel and PAHPA20, PAHPA10 and PAHPA5 coated 430SS samples in 3.5% NaCl solution

Sample	Film thickness, $\mu\text{m}$	$E_{corr}$ , V vs Ag/AgCl	$I_{corr}$ , $\mu\text{A cm}^{-2}$	$R_p$ , $\Omega\text{cm}^2$	$P$ , %*	$\eta_p$ (%)
Bare steel	—	−0.47	6.655	$7.95 \times 10^3$	—	—
PAHPA5	0.63	−0.21	1.888	$1.89 \times 10^4$	3.86	71.6
PAHPA10	0.96	−0.17	0.831	$2.56 \times 10^4$	2.81	87.5
PAHPA20	1.38	−0.27	0.187	$5.35 \times 10^4$	1.39	97.2

\*  $b_a = 0.322 \text{ V.dec}^{-1}$

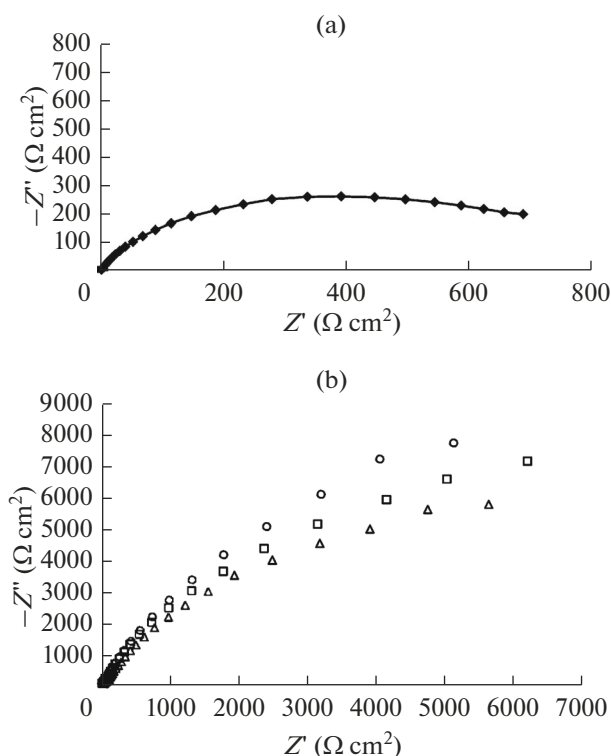


**Fig. 8.** Nyquist plots of (a) bare, (b): PHPA20 ( $\Delta$ ), PANI20 ( $\square$ ), and PAHPA20 ( $\circ$ ) coated 430SS electrodes in 3.5% NaCl.

resistance, coating resistance and charge transfer resistance, respectively.  $R_{ct}$  is related to the resistance of coating, resistance at the interface of metal and coating or the coating/solution resistance. As seen in Fig. 8, shape of EIS diagrams are similar to a depressed semicircle. Charge transfer resistance ( $R_{ct}$ ) value is equal to the semicircles diameter. The coating protection efficiency ( $\eta_z$ ) values were calculated according to the equation [31, 49]

$$\eta_z = \frac{R_{ct(c)} - R_{ct}}{R_{ct(c)}} \times 100,$$

**Table 3.** Impedance parameter values for bare and PHPA20, PAHPA20 and PANI20 coated 430SS electrodes extracted from fitting the impedance spectra to the equivalent circuit recorded in an aqueous 3.5% NaCl solution

Sample	$R_s, \Omega \text{ cm}^2$	CPE <sub>c</sub>		$R_c, \Omega \text{ cm}^2$	CPE <sub>dl</sub>		$R_{ct}, \Omega \text{ cm}^2$	$\eta_z, \%$
		$Q_c, \text{F cm}^{-2}$	$n_c^a$		$Q_{dl}, \text{F cm}^{-2}$	$n_{dl}^a$		
Blank	5.1	—	—	—	$3.70 \times 10^{-4}$	0.74	795	—
PHPA20	18.39	$1.41 \times 10^{-4}$	0.81	13599	$1.50 \times 10^{-6}$	0.79	4500	82.3
PANI20	17.32	$1.70 \times 10^{-4}$	0.82	20510	$9.50 \times 10^{-6}$	0.71	5400	85.3
PAHPA20	19.00	$1.49 \times 10^{-4}$	0.80	41500	$0.15 \times 10^{-6}$	0.81	35750	97.7

<sup>a</sup>  $n_c$  and  $n_{dl}$  indicate the capacitor like behavior of the constant phase elements  $Q_c$  and  $Q_{dl}$ .

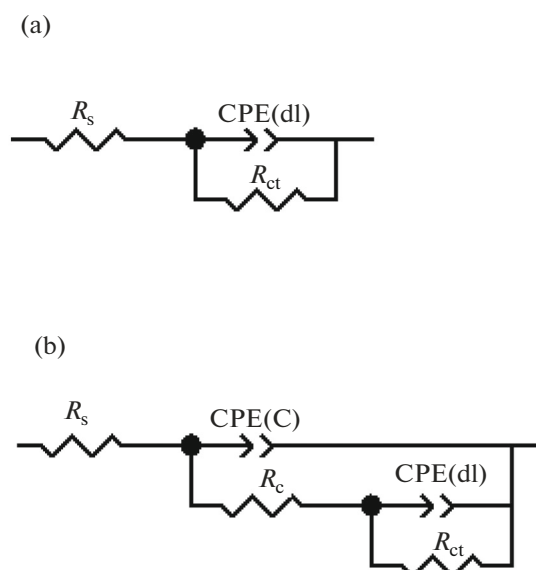


**Fig. 9.** Equivalent circuits for bare (a) and coated (b) 430SS samples.

where  $R_{ct(c)}$  and  $R_{ct}$  are the charge transfer resistance values of coated and bare samples, respectively. Table 3 depicts extracted impedance parameter values for bare and PHPA20, PANI20 and PAHPA20 coated 430SS substrates from fitting the impedance spectra to the equivalent circuit. As can be seen in this table, the  $R_{ct}$  values of coated 430SS electrodes increased from  $745 \Omega \text{ cm}^2$  for bare 430SS to  $4500 \Omega \text{ cm}^2$  for the PHPA20,  $5400 \Omega \text{ cm}^2$  for PANI20 and  $35750 \Omega \text{ cm}^2$  for PAHPA20 coated samples that shows the  $R_{ct}$  for the PAHPA20 coated electrode is the highest among all and it is about 8 times greater than  $R_{ct}$  for uncoated 430SS electrode. However, the lowest value of CPE<sub>c</sub> is that of the PANI20 ( $1.41 \times 10^{-4} \text{ F cm}^{-2}$ ), the CPE<sub>c</sub> value for PAHPA20 ( $1.41 \times 10^{-4} \text{ F cm}^{-2}$ ) is close to it. In the case of CPE<sub>dl</sub>, the lowest value is related to PAHPA20 ( $0.15 \times 10^{-6} \text{ F cm}^{-2}$ ). Low CPE and high R values are the characteristics of defect-free and uni-

**Table 4.** The EIS results of PAHPA coated 430SS samples with different thicknesses (PAHPA5, PAHPA10 and PAHPA20) in 3.5% NaCl solution

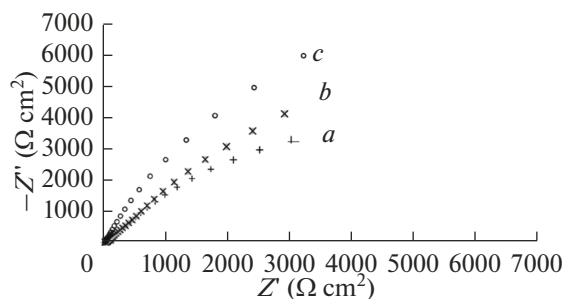
Sample	$R_s, \Omega \text{ cm}^2$	$\text{CPE}_c$		$R_c, \Omega \text{ cm}^2$	$\text{CPE}_{dl}$		$R_{ct}, \Omega \text{ cm}^2$	$\eta_z, \%$
		$Q_c, \text{F cm}^{-2}$	$n_c$		$Q_{dl}, \text{F cm}^{-2}$	$n_{dl}$		
PAHPA5	20.12	$2.61 \times 10^{-4}$	0.74	12550	$0.50 \times 10^{-6}$	0.70	3286	75.8
PAHPA10	17.07	$2.06 \times 10^{-4}$	0.69	39500	$0.28 \times 10^{-6}$	0.67	6095	86.9
PAHPA20	19.00	$1.49 \times 10^{-4}$	0.80	41500	$0.15 \times 10^{-6}$	0.81	35750	97.7

**Table 5.** The EIS results of PAHPA20 coated 430SS samples after various immersion times in 3.5% NaCl solution

Immersion time (day)	$R_s, \Omega \text{ cm}^2$	$\text{CPE}_c$		$R_c, \Omega \text{ cm}^2$	$\text{CPE}_{dl}$		$R_{ct}, \Omega \text{ cm}^2$	$\eta_z, \%$
		$Q_c, \text{F cm}^{-2}$	$n_c$		$Q_{dl}, \text{F cm}^{-2}$	$n_{dl}^a$		
3	15.04	$1.39 \times 10^{-4}$	0.82	39870	$2.63 \times 10^{-6}$	0.86	24466	96.8
5	16.41	$0.80 \times 10^{-4}$	0.80	30590	$2.05 \times 10^{-6}$	0.83	18720	95.7
10	14.66	$0.41 \times 10^{-4}$	0.86	23479	$1.40 \times 10^{-6}$	0.84	12635	93.7

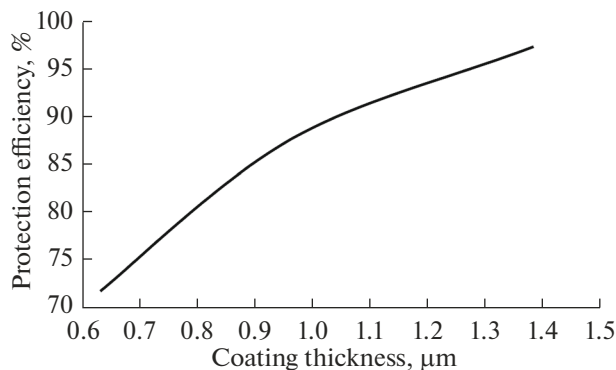
form polymer coating with excellent corrosion performance [28, 29, 46]. The higher  $R_{ct}$  values indicate that a stable passive layer is formed at the metal/polymer interface and this passive barrier layer effectively limits diffusion of the corrosive species from solution towards the underlying 430SS substrate [50]. Similar to the potentiodynamic polarization results, the highest corrosion protection is due to the copolymer. The  $\eta_z$  of PAHPA20 calculated from EIS measurements is found to be 97.7% that is in agreement with  $\eta_p$  (the protection efficiency obtained from potentiodynamic polarization data). All these results proved that the synthesized copolymer coating provide excellent protection for 430SS substrate against corrosion in the corrosive solution (3.5% wt. NaCl).

Because of the critical importance of the coating thickness in industrial applications, investigation of the copolymer film thickness and corrosion performance correlation was carried out. Figure 10 depicts impedance diagrams for 430SS electrodes coated by

**Fig. 10.** Impedance behavior of electrocopolymerized PAHPA on 430SS in 3.5% NaCl. (a) PAHPA5, (b) PAHPA10, and (c) PAHPA20.

different thickness of electrodeposited PAHPA. As can be seen in Table 4, the resistance values increase, capacitance values decrease and  $\eta_z$  improves as film thickness grows up. The calculated thickness of PAHPA5 film was  $\sim 0.6 \mu\text{m}$  and  $\eta_z$  for this film obtained about 76% which is an excellent result. The variation of the protection efficiency as a function of the electrodeposited PAHPA thickness on 430SS is shown in Fig. 11.

It is necessary for an anti-corrosion coating that remains stable and be protective against corrosion process after long exposure time to corrosive media. Figure 12 represents Nyquist plots for PAHPA20 coated 430SS electrodes after prolonged exposure time to 3.5% NaCl solution. Extracted parameters for this study are included in Table 5. These results show that PAHPA film shows superior anticorrosive behavior even after long immersion times. As the exposure

**Fig. 11.** Variation of the protection efficiency as a function of the copolymer film thickness on 430SS.



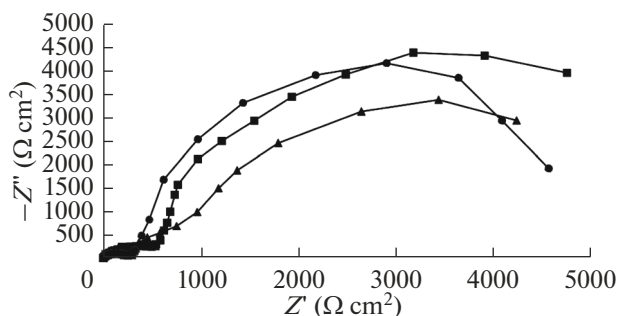


**Fig. 12.** Nyquist plots of PAHPA20 coated 430SS samples after various immersion times in 3.5% NaCl solution, 3 day (■), 5 days (●), and 10 days (▲).

time increases from 1 h to 3 day, corrosion protection efficiency ( $\eta_z$ ) decreases from 97.7 to 96.8% which this decreasing is very slight. The  $\eta_z$  value decreases very slowly and after 10 days, its value is  $\sim 94\%$ . Comparing these results with our previous work [19], indicates that aniline/4-hydroxy phenyl acetic acid copolymer film on the 430SS electrode after 5 day exposure time to 3.5% NaCl solution, has better protection efficiency from polyaniline coating on the same electrode and in the same conditions.

## CONCLUSIONS

Electrochemical deposition of poly(aniline-co-4-hydroxy phenyl acetic acid) (PAHPA) by cyclic voltammetry using aqueous oxalic acid 0.3 M solution as reaction medium, on ferritic and economic 430 Stainless Steel surface, yields nanostructure, uniform and electrochemically stable film. Our corrosion protection evaluations revealed that PAHPA coated 430SS shows excellent corrosion resistance in the highly corrosive solutions like 3.5% NaCl in comparison with polyaniline and poly(4-hydroxy phenyl acetic acid) coated samples. Long time immersion test revealed that, protection efficiency of PAHPA20 coated 430SS electrode decreases very slowly and after 10 days, protection efficiency is  $\sim 94\%$ .

## REFERENCES

- Iroh, J.O. and Su, W., *Electrochim. Acta.*, 2000, vol. 46, p. 15.
- Sathiyarayanan, S., Devi, S., and Venkatachari, G., *Prog. Org. Coat.*, 2006, vol. 56, p. 114.
- Elia, L.F.D., Ortiz, R.L., Marquez, O.P., Marquez, J., and Martinez, Y., *J. Electrochem. Soc.*, 2001, vol. 148, p. 297.
- MacDiarmid, A.G., Chiang, J.C., and Richter, A.F., *Synth. Met.*, 1987, vol. 18, p. 393.
- Girard, F., Ye, S., Laperriere, G., and Belanger, D., *J. Electroanal. Chem.*, 1992, vol. 334, p. 35.
- Ingnas, O. and Admassie, S., *Adv. Mater.*, 2014, vol. 26, p. 830.
- Nguyen, M.T. and Deo, L.H., *J. Electrochem. Soc.*, 1989, vol. 136, p. 2131.
- Chen, S.M., Ramachandran, R., Mani, V., and Saraswathi, R., *Int. J. Electrochem. Sci.*, 2014, vol. 9, p. 4072.
- Wang, K., Wu, H.P., Meng, Y.N., and Wei, Z.X., *Small*, 2014, vol. 10, p. 14.
- Thakur, B., Amarnath, C.A., Mangoli, S.H., and Sawant, S.N., *Sens. Actuators, B*, 2015, vol. 207, p. 262.
- Tian, Y., Qu, K., and Zeng, X., *Sens. Actuators, B*, 2017, vol. 249, p. 423.
- Xue, L., Wang, W., Liu, G., and Wan, P., *Sens. Actuators, B*, 2017, vol. 244, p. 47.
- Xu, X.J., Liu, R.H., and Li, L.D., *Chem. Commun.*, 2015, vol. 51, p. 16733.
- Nakajima, T. and Kawagoe, T., *Synth. Met.*, 1989, vol. 28, p. 629.
- Kozarenko, O.A., Dyadyun, V.S., Papakin, M.S., Posudievsky, O.Y., Koshechko, V.G., and Pokhodenko, V.D., *Electrochim. Acta.*, 2015, vol. 184, p. 111.
- Poopathy, K. and Qayyum, M.M.B., *J. Electrochem. Soc.*, 1994, vol. 141, p. 147.
- Pan, T.J., Zuo, X.W., Wang, T., Hu, J., Chen, Z.D., and Ren, Y.J., *J. Power Sources*, 2016, vol. 302, p. 180.
- Sazou, D., Kourouzidou, M., and Pavlidou, E., *Electrochim. Acta.*, 2007, vol. 52, p. 4385.
- Farhadi, K., Zebhi, H., Najafi Moghadam, P., Es'haghi, M., and Ashassi-Sorkhabi, H., *Synth. Met.*, 2014, vol. 195, p. 29.
- Chaudhari, S. and Patil, P.P., *J. Appl. Polym. Sci.*, 2007, vol. 106, p. 400.
- Duran, B., Bereket, G., Turhan, M.C., and Virtanen, S., *Thin Solid Films*, 2011, vol. 519, p. 5868.
- Ozyilmaz, A.T., Ozyilmaz, G., and Colak, N., *Surf. Coat. Technol.*, 2006, vol. 201, p. 2484.
- Wang, W., Zhu, F., Dai, Y., Zhang, H., and Lei, J., *Int. J. Electrochem. Sci.*, 2016, vol. 11, p. 4000.
- Xu, J., Zhang, Y., Zhang, D., Tang, Y., and Cang, H., *Prog. Org. Coat.*, 2015, vol. 88, p. 84.
- Heydari, M.H., Zebhi, H., Farhadi, K., and Najafi Moghadam, P., *Synth. Met.*, 2016, vol. 220, p. 78.
- Chen, F. and Liu, P., *Appl. Mater. Interfaces*, 2011, vol. 3, p. 2694.
- Shabani-Nooshabadi, M., Ghoreishi, S.M., and Behpour, M., *Corros. Sci.*, 2011, vol. 53, p. 3035.
- Munoz, A.I., Anton, J.G., Guinon, J.L., and Herranz, V.P., *Corros. Sci.*, 2007, vol. 49, p. 3200.
- Mrad, M., Dhoubi, L., and Triki, E., *Synth. Met.*, 2009, vol. 159, p. 1903.
- Kilmartin, P.A., Trier, L., and Wright, G.A., *Synth. Met.*, 2002, vol. 131, p. 99.
- Kamaraj, K., Karpakam, V., Sathiyarayanan, S., and Venkatachari, G., *Mater. Chem. Phys.*, 2010, vol. 122, p. 123.
- Maouche, N. and Nessark, B., *Corrosion*, 2008, vol. 64, p. 315.
- Shabani-Nooshabadi, M., Ghoreishi, S.M., Jafari, Y., and Kashanizadeh, N., *J. Polym. Res.*, 2014, vol. 21, p. 416.
- Zhong, L., Zhu, H., Hu, J., Xiao, S.H., and Gan, F.X., *Electrochim. Acta.*, 2006, vol. 51, p. 5494.

35. Hermas, A.A., *Prog. Org. Coat.*, 2008, vol. 61, p. 95.
36. Shabani-Nooshabadi, M., Mollahoseiny, M., and Jafari, Y., *Surf. Interface Anal.*, 2014, vol. 46, p. 472.
37. Lu, H., Zhou, Y., Vongehr, S., Hu, K., and Meng, X., *Synth. Met.*, 2011, vol. 161, p. 1368.
38. Bereket, G., Hur, E., and Sahin, Y., *Prog. Org. Coat.*, 2005, vol. 54, p. 63.
39. Narayanasamy, B. and Rajendran, S., *Prog. Org. Coat.*, 2010, vol. 67, p. 246.
40. Yagan, A., Pekmez, N.O., and Yildiz, A., *J. Electroanal. Chem.*, 2005, vol. 578, p. 231.
41. Qiu, H.J., Wan, M.X., Matthews, B., and Dai, L.M., *Macromolecules*, 2001, vol. 34, p. 675.
42. Liu, J.M. and Yang, S.C., *J. Chem. Soc., Chem. Commun.*, 1991, vol. 21, p. 1529.
43. Long, Y.Z., Chen, Z.J., Zheng, P., Wang, N.L., Zhang, Z.M., and Wan, M.X., *J. Appl. Phys.*, 2003, vol. 93, p. 2962.
44. Zhang, L.J. and Wan, M. X., *Nanotechnology*, 2002, vol. 13, p. 750.
45. Wei, Z.X. and Wan, M.X., *J. Appl. Polym. Sci.*, 2003, vol. 87, p. 1297.
46. Huang, K. and Wan, M.X., *Chem. Mater.*, 2002, vol. 14, p. 3486.
47. Ozyilmaz, A.T., Erbil, M., and Yazici, B., *Prog. Org. Coat.*, 2004, vol. 51, p. 47.
48. Zeybek, B., Pekmez, N.O., and Kilic, E.; *Electrochim. Acta.*, 2011, vol. 56, p. 9277.
49. Chaudhari, S., Sainkar, S.R., and Patil, P.P., *J. Phys. D: Appl. Phys.*, 2007, vol. 40, p. 520.
50. Pawar, P., Gaikawad, A.B., and Patil, P.P., *Sci. Technol. Adv. Mater.*, 2006, vol. 7, p. 732.